



Tree Physiology 31, 1128–1141
doi:10.1093/treephys/tpr094

Research paper

Tree size and light availability increase photochemical instead of non-photochemical capacities of *Nothofagus nitida* trees growing in an evergreen temperate rain forest

Rafael E. Coopman^{1,8}, Verónica F. Briceño², Luis J. Corcuera³, Marjorie Reyes-Díaz^{4,5}, Daniela Alvarez^{4,5}, Katherine Sáez^{4,5}, José I. García-Plazaola⁶, Miren Alberdi^{4,5} and León A. Bravo^{5,7}

¹Forest Ecophysiology Laboratory, Facultad de Ciencias Forestales y Recursos Naturales, Universidad Austral de Chile, Independencia 641, Casilla 567, Valdivia, Chile; ²Research School of Biology, Division of Ecology, Evolution and Genetics, Australian National University, Canberra, ACT 0200, Australia; ³Departamento de Botánica, Facultad de Ciencias Naturales y Oceanográficas, Universidad de Concepción, Casilla 160-C, Concepción, Chile; ⁴Departamento de Ciencias Químicas y Recursos Naturales, Universidad de La Frontera, Casilla 54-D, Temuco, Chile; ⁵Center of Plant-Soil Interaction and Natural Resources Biotechnology, Scientific and Technological Bioresource Nucleus (BIOREN), Universidad de La Frontera, Casilla 54-D, Temuco, Chile; ⁶Departamento de Biología Vegetal y Ecología, Universidad del País Vasco UPV/EHU, Apdo. 644, E-48080 Bilbao, Spain; ⁷Laboratorio de Fisiología y Biología Molecular Vegetal, Departamento de Ciencias Agronómicas y Recursos Naturales, Facultad de Ciencias Agropecuarias y Forestales, Universidad de La Frontera, Casilla 54-D, Temuco, Chile; ⁸Corresponding author (rafael.coopman@docentes.uach.cl)

Received March 10, 2011; accepted August 11, 2011; handling Editor Ülo Niinemets

Nothofagus nitida (Phil.) Krasser (Nothofagaceae) regenerates under the canopy in microsites protected from high light. Nonetheless, it is common to find older saplings in clear areas and adults as emergent trees of the Chilean evergreen forest. We hypothesized that this shade to sun transition in *N. nitida* is supported by an increase in photochemical and non-photochemical energy dissipation capacities of both photosystems in parallel with the increase in plant size and light availability. To dissect the relative contribution of light environment and plant developmental stage to these physiological responses, the photosynthetic performance of both photosystems was studied from the morpho-anatomical to the biochemical level in current-year leaves of *N. nitida* plants of different heights (ranging from 0.1 to 7 m) growing under contrasting light environments (integrated quantum flux (IQF) 5–40 mol m⁻² day⁻¹). Tree height (TH) and light environment (IQF) independently increased the saturated electron transport rates of both photosystems, as well as leaf and palisade thickness, but non-photochemical energy flux, photoinhibition susceptibility, state transition capacity, and the contents of D1 and PsbS proteins were not affected by IQF and TH. Spongy mesophyll thickness and palisade cell diameter decreased with IQF and TH. A_{max} , light compensation and saturation points, Rubisco and nitrogen content (area basis) only increased with light environment (IQF), whereas dark respiration (R_d) decreased slightly and relative chlorophyll content was higher in taller trees. Overall, the independent effects of more illuminated environment and tree height mainly increased the photochemical instead of the non-photochemical energy flux. Regardless of the photochemical increase with TH, carbon assimilation only significantly improved with higher IQF. Therefore it seems that mainly acclimation to the light environment supports the phenotypic transition of *N. nitida* from shade to sun.

Keywords: NPQ components, ontogeny, PSII and PSI light energy partitioning, state transitions.

Introduction

Shade-tolerant and semi-tolerant tree species experience diverse light conditions during their lifetime, starting as germinants on the extreme shaded forest floor but often gaining

access to the well-lit canopy layer at maturity (Poorter et al. 2005, Coopman et al. 2008). In tropical rain forests, there is a well-defined vertical gradient of light availability, where trees find brighter light conditions as they increase in height (Poorter

et al. 2005). However, in several forests the formation and closure of canopy openings of different dimensions determine spatial and temporal heterogeneous light environments (Chazdon and Fetcher 1984). Strong early environmental requirements in combination with high mortality rates determine when, where and under what conditions tree seedlings are found (Grubb 1977, Kozlowski 2002). Besides, several forest tree species change their light requirements in different developmental stages (Poorter et al. 2005, Lusk et al. 2008, Coopman et al. 2008, 2010, Alberdi et al. 2009, Reyes-Díaz et al. 2009). Therefore the light stress level experienced by forest trees depends on two factors that vary at a specific tree ontogenetic stage: light availability and light requirements.

As has been commonly reported, leaf morphology, among other factors, is determined by the daily amount of light received during growth and foliar development. Thus, typical structural and biochemical leaf features of sun plants relative to shade plants are lower leaf area, specific leaf area (SLA) and chlorophyll/dry weight ratio, and higher biomass, nitrogen content and Rubisco (ribulose 1,2 biphosphate carboxylase-oxygenase) content (Givnish 1988, Evans 1989, Lawlor 2001, Meziane and Shipley 2001, Larcher 2003, Wright et al. 2004). However, several studies reported that physiology can differ with tree size or age. Specifically, early ontogenetic increases in photosynthetic capacity and related traits have been reported in relatively shade-tolerant deciduous tree species, which peaked approximately at the size of reproductive onset (Thomas 2010). Ishida et al. (2005) reported that photosynthetic capacity was higher in saplings than in seedlings of the pioneer tree *Macaranga gigantea*, and this ontogenetic change was not related to light availability. In agreement, Kenzo et al. (2006) found that the photosynthetic capacity of dipterocarp trees depends on tree height, and suggested, like other authors, that tree species have different photosynthetic capacities according to their growth stage, to the light conditions or to both factors, as a result of differences in leaf structure and biochemistry (Björkman 1981, Lambers et al. 2008). Therefore, efficient light utilization depends on how plants are able to handle the absorbed energy in a safe manner, avoiding photoinhibition and maximizing photochemical light utilization in carbon gain. This can only be reached if light capture, light partitioning and photoprotection are finely tuned at molecular (Pascal et al. 2005), physiological (Ensminger et al. 2006) and morpho-anatomical (Ishida et al. 2005) levels with the use of available resources during plant ontogeny.

Nothofagus nitida (Phil.) Krasser is a canopy emergent species of the Chilean evergreen forest. It often regenerates successfully under the canopy at low light availabilities, behaving similarly to very shade-tolerant species, such as *Podocarpus nubigena* and *Laureliopsis philippianan* (Lusk et al. 2006). It is also found in gaps or forest edges where the regeneration begins in shady microsites. For this reason, it is commonly found among shrubs, ferns and other small vegetation, tree stumps, exposed root

systems, and fallen trees located near the forest floor. In these locations, as plants grow and cross the first canopy cover, they are progressively exposed to more light (Kira and Yoda 1989, Coopman et al. 2010). Hence, older seedlings (around 1 m tall) may grow in more light-exposed sites with *Drimys winteri* and *Ecryphia cordifolia*, two sun species (Donoso 1993, Veblen et al. 1996). This suggests that as *N. nitida* develops, it acquires the capacity to grow in more illuminated environments. In this way, *N. nitida* changes from an obligate umbrophyllous species at the recruiting phase to a facultative umbrophyllous species during its juvenile growth phase (Coopman et al. 2008, 2010). Research in size-dependent changes in forest plants is a relatively recent issue (Bond 2000, Reich 2001, Coopman et al. 2008, 2010, Lusk et al. 2008). Therefore, research that deals with photoprotective mechanism variations with tree size is even scarcer (Ishida et al. 2005, Coopman et al. 2008, 2010, Reyes-Díaz et al. 2009). In a previous work, we have demonstrated that the partitioning of absorbed energy to photochemical and non-photochemical paths in *N. nitida* seedlings up to 0.4 m tall was primarily affected by light environment; in contrast, the light absorption capacity depends on both seedling developmental stage and environment (Coopman et al. 2010). In this work we expanded the ontogenetic range previously considered focusing on the seedling–sapling transition in *N. nitida* plants from 0.1 to 7 m growing in their natural heterogeneous light environment. Our main objective was to clarify the relative contribution of light environment and plant size to light energy partitioning (photochemical processes versus non-photochemical energy dissipation), CO₂ assimilation and susceptibility to photoinhibition during this transition.

We postulate that the photosynthetic capacity and non-photochemical photoprotective mechanisms increase with plant size and light availability. In order to test this hypothesis and with the aim of distinguishing between the effects of ontogeny and light environment on the functioning of photosynthetic apparatus, we have used a hierarchical partitioning procedure to study the photosynthetic performance and photoprotection in both photosystems of *N. nitida* leaves from plants of different heights (0.1–7 m) growing within a range of light availabilities (integrated quantum flux (IQF) 5–40 mol m⁻² day⁻¹). Additionally, we explored several leaf attributes associated with their photosynthetic performance such as changes in leaf morpho-anatomy, nitrogen content and photosynthetic proteins (thylakoid polypeptides and Rubisco contents) in order to explain potential functional changes observed with plant size and light availability.

Materials and methods

Study site

The study was carried out at the beginning of January 2008 at Katalapi Park, which is located in Pichiquillaípe, Xth Region, in

South Central Chile (41°31'07.5" S, 72°45'2.2" W). This area experiences a temperate maritime climate, where the annual mean precipitation is around 2000 mm, without dry months. The lowest air temperature reached $-5\text{ }^{\circ}\text{C}$ in June, but subzero temperatures also occurred during autumn and at the beginning of spring. The mean maximum air temperature ranged between 10 and 22 $^{\circ}\text{C}$ in July and January, respectively. Annual maximum photosynthetic photon flux densities (PPFDs) of $\sim 2150\ \mu\text{mol m}^{-2}\text{ s}^{-1}$ occurred in December. Climatic details for the study area are shown in Coopman et al. (2010).

Forest structure and light environments

The study site was a 5-ha secondary forest stand with some remnant *N. nitida* seed trees. The site has been protected from anthropogenic alterations for ~ 25 years. At present, the regeneration is heterogeneously distributed in the area and dominated by a variety of sun species like *D. winteri*, *Embothrium coccineum*, *E. cordifolia* and *N. nitida*, where the taller individuals reach up to 10 m. The previous situation creates a high variation in light availability that supports seedlings and saplings of mixed species growth. Light availability at the apex of each plant was quantified by hemispherical photography, using a Coolpix 4500 digital camera (Nikon Co., Japan) with an FCE8 fish-eye lens of 182° field of view (Nikon Co., Japan). Photographs were taken under homogeneous diffuse sky light conditions. The resulting photographs were analysed for daily integrated quantum flux transmitted through the canopy (IQF = direct + diffuse quantum fluxes) with the Gap Canopy Analyzer 2.0 software (Frazer et al. 1999). A total of 120 *N. nitida* plant heights and light environments were initially measured. From this sample, in order to explore the effects of entire plant heights and light availability ranges, 35 plants of different heights (0.1–6.5 m, corresponding to a range of 1–16-year-old plants) growing at different IQF availabilities (5–40 $\text{mol m}^{-2}\text{ day}^{-1}$) were selected and marked (Figure 1). Physiological, morpho-anatomical (structural) and biochemical features were studied in new fully expanded (first year) leaves collected from the top of the plant foliage. Biochemical and morpho-anatomical determinations were made on equivalent samples immediately after photosynthetic measurements.

Net photosynthesis

Net CO_2 assimilation at different light intensities (1500, 1000, 500, 300, 200, 100, 75, 50, 25, 10, 5 and 0 $\mu\text{mol photons m}^{-2}\text{ s}^{-1}$) was measured in vivo with an infrared gas analyser (Ciras-2, PP Systems, UK). The CO_2 reference concentration was 380 ppm, with a flow rate of 200 ml min^{-1} and 75% relative humidity inside the leaf chamber. The temperature inside the leaf chamber was maintained at $15 \pm 2\text{ }^{\circ}\text{C}$. This value was obtained in previous determinations, at different temperatures, indicating that 15 $^{\circ}\text{C}$ is within the range of the optimum temperature for photosynthesis in this species. Light compensation point (LCP),

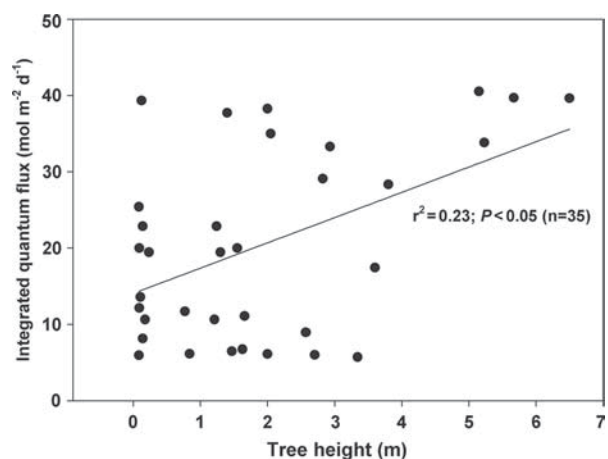


Figure 1. Relationship between light availability and tree height of *N. nitida* individuals growing in a Chilean evergreen rain forest. Light availability was expressed as integrated quantum flux derived from a hemispherical photograph. The determination coefficient, P level and numbers of individuals are given.

light saturation point (LSP), maximal rate of net CO_2 assimilation (A_{max}) and dark respiration (R_d) were calculated with the Photosynthesis Assistant software 1.1 (Dundee Scientific, Dundee, UK). Instantaneous water use efficiency (WUE_i) and photosynthetic nitrogen use efficiency (PNUE) were calculated as $\text{WUE}_i = A_{\text{sat}}/T_{\text{sat}}$ and $\text{PNUE} = A_{\text{sat}}/N$, where A_{sat} and T_{sat} are saturated assimilation and transpiration rates measured at 665 $\mu\text{mol photons m}^{-2}\text{ s}^{-1}$ and N is leaf nitrogen content (mol m^{-2}). All measurements were performed from 09:00 to 13:00 h. In case the leaf did not cover the entire leaf cuvette surface (2.5 cm^2), a digital photograph of the leaf was taken immediately after the measurement in order to estimate the actual leaf area using SigmaScan Pro 5.0 software (SPSS Inc., USA). Gas exchange values given by CIRAS-2 were corrected using the cuvette area/actual leaf area ratio as a correction factor.

Chlorophyll fluorescence and P700 measurements

Light response curves of chlorophyll a fluorescence and P700 redox state assessment were performed simultaneously with a Dual-PAM-100 measuring system (Walz, Effeltrich, Germany) in detached new fully expanded leaves. Leaves were immediately dark adapted for 30 min (to obtain open reaction centres). A saturating pulse was applied to obtain F_m ; then, leaves were exposed for 5 min at each PPFD (0, 27, 58, 131, 221, 344, 435, 665, 1033 and 1957 $\mu\text{mol m}^{-2}\text{ s}^{-1}$) in order to obtain steady-state readings. All measurements were performed at 15 $^{\circ}\text{C}$. Temperature was controlled with a water jacket system placed around the Dual-D leaf holder connected to a thermoregulated water bath. Leaf temperature was monitored with a fine wire K-type thermocouple (Sper Scientific Ltd, Scottsdale, AZ, USA). Recordings and calculations were performed with the Dual-PAM 1.7 data analysis and control software (Walz, Effeltrich, Germany).

The saturation pulse method originally developed for chlorophyll fluorescence quenching analysis (Schreiber et al. 1986) was used for assessment of PSI quantum yields (Klughammer and Schreiber 1994). Analysis of PSI was based on a routine for assessment of the maximal P700 change (Pm determination), which involves pre-illumination with far-red light for 2 s ($\sim 117 \mu\text{mol photons m}^{-2} \text{s}^{-1}$) and a saturation pulse ($9000 \mu\text{mol photons m}^{-2} \text{s}^{-1}$) that induces maximal P700 oxidation followed by full reduction. The Pm determination is analogous to Fo and F_m determinations. The concept of excitation energy partitioning originally conceived for PSII by Demmig-Adams et al. (1996) was adopted for PSI. Hence, saturated PSII effective photochemical quantum yield [$\Phi(\text{II})$], yield of energy dissipation by antenna down-regulation [$\Phi(\text{NPQ})$], where NPQ refers to non photochemical quenching and constitutive non-photochemical energy dissipation plus fluorescence of PSII [$\Phi(\text{NO})$] were calculated according to Kramer et al. (2004). Besides, PSI effective photochemical quantum yield [$\Phi(\text{I})$] and the yields of non-photochemical quenching caused by donor [$\Phi(\text{ND})$] and acceptor [$\Phi(\text{NA})$] side limitations were obtained at saturating PPFD. Finally, to determine the light energy flux rates consumed at PSII and PSI by photochemical and non-photochemical processes, we calculated energy fluxes in the same way as for electron transport rate through photosystem II (Hendrickson et al. 2004). For example, $J_{(\text{NPQ})} = \Phi(\text{NPQ}) \times \text{PPFD}_{\text{sat}} \times 0.5 \times 0.84$, where PPFD_{sat} is $665 \mu\text{mol m}^{-2} \text{s}^{-1}$; the factor 0.5 corrects the expression by the assumption that the efficiency of the two photosystems is equal and that light is equally distributed between them and 0.84 is the leaf absorptance. No specific leaf absorptance measurement for *N. nitida* was carried out and the factor 0.84 was considered as the mean value of absorptance for green leaves (Demmig-Adams et al. 1987). In this way, we determine the capacity for the following light energy fluxes towards photochemistry [$J_{(\text{II})}$ and $J_{(\text{I})}$], ΔpH -xanthophyll-regulated thermal dissipation [$J_{(\text{NPQ})}$], the sum of fluorescence quenching and constitutive thermal dissipation [$J_{(\text{NO})}$], and the non-photochemical fluxes consumed by donor [$J_{(\text{ND})}$] and acceptor [$J_{(\text{NA})}$] side limitations.

Non-photochemical quenching components determinations

NPQ components were determined in detached new fully expanded leaves at 15°C . These measurements were performed using a pulse-amplitude modulated fluorometer (FMS 2, Hansatech Instruments Ltd, King's Lynn, UK). Non-photochemical quenching was resolved into a slow-relaxing component of NPQ (NPQ_s) and a fast-relaxing component of NPQ (NPQ_f) essentially as described by Walters and Horton (1991). The protocol used was the application of $2000 \mu\text{mol photons m}^{-2} \text{s}^{-1}$ of actinic light for 2 h provided by an LS2 white light source (Hansatech Instruments Ltd) connected to an LD2/3 electrode chamber. Then, the actinic light was turned off and the dark recover kinetic during 1 h was

analysed. During this time saturating pulses to obtain F_m were applied. $\text{NPQ}_s = (F_m - F_m^r)/F_m^r$ and $\text{NPQ}_f = (F_m/F_m') - (F_m/F_m^r)$. F_m^r (the value of F_m that would have been attained if only slowly relaxing quenching had been present in the light) was obtained by extrapolation of the data points recorded towards the end of the relaxation back to the time when the actinic light was removed in a semi-logarithmic plot of maximum fluorescence yield versus time. The relative capacity for state 1–state 2 transitions was estimated as described in Lunde et al. (2000), using a pulse-amplitude modulated fluorometer (FMS 2, Hansatech Instruments Ltd). The instrument was equipped with a blue light source consisting of an LS2 white light source (Hansatech Instruments Ltd) with a Corning 4-96 filter ($\sim 80 \mu\text{mol photons m}^{-2} \text{s}^{-1}$) and far-red light ($\lambda = 735 \text{ nm}$, $20 \mu\text{mol photons m}^{-2} \text{s}^{-1}$) provided by the FMS 2 fluorometer (Hansatech Instruments Ltd). Relative state transitions (Fr) were calculated as $\text{Fr} = [(F_i' - F_i) - (F_{ii}' - F_{ii})]/(F_i' - F_i)$, where F_i' and F_{ii}' designate fluorescence in the absence of PSII light in state 1 and state 2, respectively (Lunde et al. 2000).

Leaf anatomy

Samples of leaf lamina (avoiding large veins) of the 35 plants were cut and immediately fixed in formalin–acetic acid–alcohol. The leaf pieces were post-fixed in 2% osmium tetroxide for ~ 1 h before being dehydrated in an ethanol series and propylene oxide, and then embedded in epoxy resin. Transverse sections (90–100 nm thickness) were cut with a glass knife mounted in an ultramicrotome (MT2-B, Dupont Instruments, Cincinnati, OH, USA) and double stained with a solution of 1% safranin and 1% gentian violet in water for light microscopy. Digital images (3840×3072 pixels) were taken using an ACT video camera attached to an Axioplan-2 microscope (Carl Zeiss, Oberkochen, Germany). Anatomical dimensions were obtained from image measurements done with SigmaScan Pro software version 5.0 (SPSS Inc., Chicago, IL, USA). Porosity was calculated from the ratio of the total area of air spaces to the area between both epidermal cell layers.

Specific leaf area, leaf nitrogen content and relative chlorophyll content

Twenty new fully expanded leaves from each of the 35 plants were cut and wrapped in moist paper and conserved in a cool box, until further processing after 24 h. In the laboratory they were rehydrated according to the protocol of Garnier et al. (2001). Leaf area was determined by a photographic method using SigmaScan Pro 5 software (SPSS Inc.). Leaf dry mass was obtained after 2 days of drying at 70°C . Specific leaf area was calculated as the ratio of leaf area/dry weight. Nitrogen content was evaluated in the same leaves used for SLA determinations. We used the Kjeldahl method as described by Sadzawka et al. (2004). Briefly, digestion involved 95–97%

sulphuric acid (H_2SO_4) including potassium sulphate (K_2SO_4) and pentahydrated copper sulphate ($\text{CuSO}_4 \cdot 5\text{H}_2\text{O}$) as catalyst. Samples were distilled to recover NH_3 and then titrated with 40% boric acid (H_3BO_3) and 32% sodium hydroxide (NaOH) using red methyl and green bromocresol dissolved in 96% ethanol as indicators. Relative chlorophyll content was measured as SPAD values in the same 20 leaves per plant with the chlorophyll meter SPAD-502 (Minolta Camera Co., Tokyo, Japan) avoiding placing the meter over major leaf veins. The SPAD-502 meter provided reliable estimates of relative leaf chlorophyll (Markwell et al. 1995, Richardson et al. 2002).

Thylakoid polypeptide analyses

Four samples of leaf tissue (~0.1 g fresh weight) from individual plants were frozen in liquid nitrogen. Thylakoidal proteins were extracted and analysed as per Spangfort and Andersson (1989) and an aliquot of the final extract was kept to measure chlorophyll content according to Arnon et al. (1949) to determine extraction yields and standardize gel loading. Four samples were analysed by sodium dodecyl sulphate-polyacrylamide gel electrophoresis under denaturing conditions in 15% polyacrylamide mini-gels containing 6 M urea, according to Laemmli (1970). An equivalent of 6 μg chlorophyll was loaded on each gel lane. In the case of D1, three lanes were loaded with 1.25, 2.5 and 3.75 pmol of D1 standard protein (AS01-016S, AgriSera, Vännäs, Sweden). After the electrophoresis, the gels were electrotransferred to nitrocellulose membranes and blocked with 5% non-fat milk. After blocking, the membranes were incubated with polyclonal antibodies against light harvesting complex (Lhc) polypeptides (anti-LhcA1, -LhcA2, -LhcA3, -LhcA4, -LhcB1, -LhcB2, -LhcB3, -LhcB4, -LhcB5 and -LhcB6) 1:10,000 and anti-PsbA (D1) and PsbS 1:5000 (AgriSera) dilutions in Tween Tris-buffered saline (0.1% Tween-20, 20 mM Tris-HCl, 500 mM NaCl; TTBS) plus 2% non-fat milk for 1 h at room temperature in an orbital shaker. The three membranes were washed three times for 10 min with TTBS. Incubation with the secondary antibody conjugated with horseradish peroxidase (Amersham-Pharmacia Biotech, Uppsala, Sweden) at 1:2000 dilution was carried out. Blots were developed using Lumi-Phos WB chemiluminescent reagent (Pierce, Rockford, IL, USA) on X-ray film (Fuji, Tokyo, Japan). Quantitative densitometry of D1 and relative intensity of LHC polypeptides and PsbS (no standard protein was available) chemiluminescent bands produced on four western blot X-ray films were quantified and averaged using the program SigmaScan Pro 5.0 (Systat Software Inc., San Jose, CA, USA).

Statistics

Multiple linear regression analysis was conducted to assess the relationship between functional, structural and biochemical leaf traits with light availability (IQF) and tree height (TH). In

order to detect changes in light energy partitioning and gas exchange capacities induced by IQF and TH, we used light-saturated values ($665 \mu\text{mol photons m}^{-2} \text{ s}^{-1}$) in the multiple linear regression analysis. A hierarchical partitioning procedure was used to quantify the contribution (independent determination coefficient) of each predictor variable to the total explained variance by the regression models (Chevan and Sutherland 1991). Model assumptions were checked for normality ($P < 0.05$), homogeneity of variances ($P < 0.05$), independence (Durbin-Watson statistic difference from $2 < 0.5$) and co-linearity [variance inflation factor ($\text{VIF} < 4$)] (Sokal and Rohlf 1995, Quinn and Keough 2006). If the data did not meet the assumptions, response variable transformation proceeded. All the statistical analyses were performed with SigmaStat 3.1 software (Systat Software Inc., San Jose, CA, USA).

Results

Relationship between IQF and TH

In the understorey (up to ~3.5 m TH), IQF varied between 3.98 and 40.53 mol photons $\text{m}^{-2} \text{ day}^{-1}$, corresponding to 6.6–78.5% of canopy openness (Figure 1). On the other hand, upper leaves of taller trees (3.5–6.5 m TH) were exposed only to the brighter range of light availabilities. Hence, these trees received an IQF between 28.00 and 40.53 mol photons $\text{m}^{-2} \text{ day}^{-1}$, corresponding to 41.4–78.5% of canopy openness. A weak positive relationship between IQF and TH was found in the selected sample ($n = 35$; $r^2 = 0.23$; $P < 0.05$), allowing the insertion of these two predictor variables into a model with permissible levels of co-linearity ($\text{VIF} < 4.0$) (Figure 1).

Effect of IQF and TH on relative chlorophyll content and CO_2 assimilation light response curve parameters

Relative chlorophyll content was affected by IQF and TH ($P < 0.001$), which explained 46% of its variance (Figure 2a). Chlorophyll decreased with IQF ($P < 0.001$), which explained 9% of its variation. Hence, shadier trees showed 15% higher chlorophyll than more light-exposed trees ($P < 0.001$). Conversely, chlorophyll increased with TH ($P < 0.001$), which explained 37% of its variation (Figure 2a). Hence, small seedlings showed an 11% lower relative chlorophyll content than tallest trees. None of the parameters derived from light response curves of CO_2 assimilation were affected by TH (lowest $P < 0.148$) (Figure 2b–f). In contrast, LCP ($P = 0.01$), LSP ($P = 0.005$) and A_{max} ($P < 0.001$) increased with IQF, where IQF explained 19, 26 and 34% of its variations, respectively (Figure 2c–e), while R_d slightly decreased with IQF ($P = 0.039$), which explained 15% of its variation (Figure 2b). Instantaneous water use efficiency and PNUE were related to neither TH nor IQF (see Table S2, available as Supplementary Data at *Tree Physiology* Online).

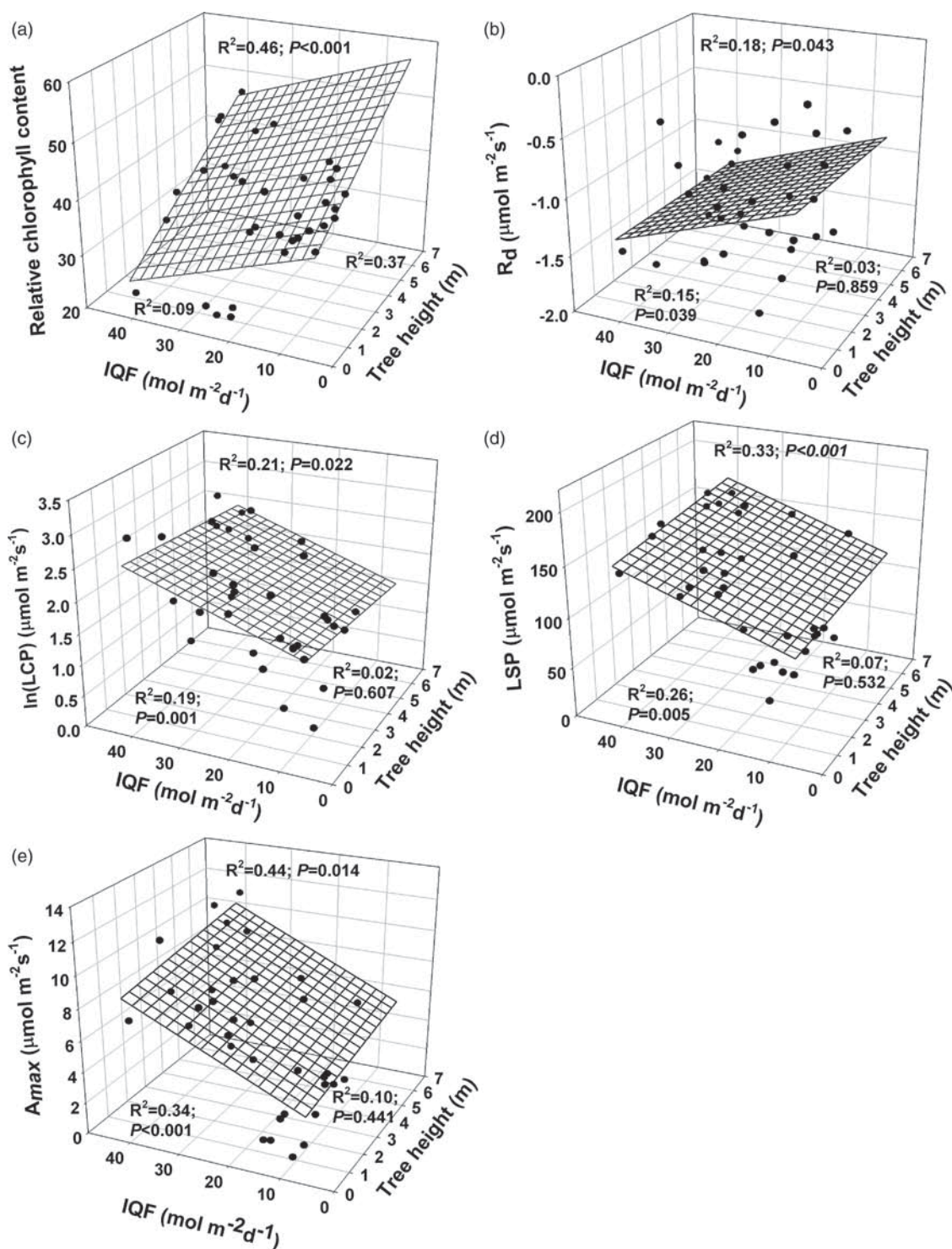


Figure 2. Integrated quantum flux and tree height effects on relative chlorophyll content and CO_2 assimilation light response curve parameters of *N. nitida* individuals growing in a Chilean evergreen rain forest. (a) Relative chlorophyll content, (b) dark respiration (R_d), (c) light compensation point (LCP), (d) light saturation point (LSP) and (e) maximal net photosynthetic rate (A_{max}). P level of regression, and model and partial determination coefficients are given. Partial P values for IQF and tree size are shown when one variable is non-significant.

Effect of IQF and TH on chlorophyll fluorescence and P700 assessment light response curves

Photochemical energy flux capacities of both photosystems [$J_{(II)}$ and $J_{(I)}$] increased with IQF and TH ($P < 0.001$), which

together explained 67 and 69% of its variation, respectively (Figure 3a and b). Besides, $J_{(II)}$ and $J_{(I)}$ were affected by TH ($P < 0.001$), which explained 34 and 36% of the increases. Integrated quantum flux was responsible for the

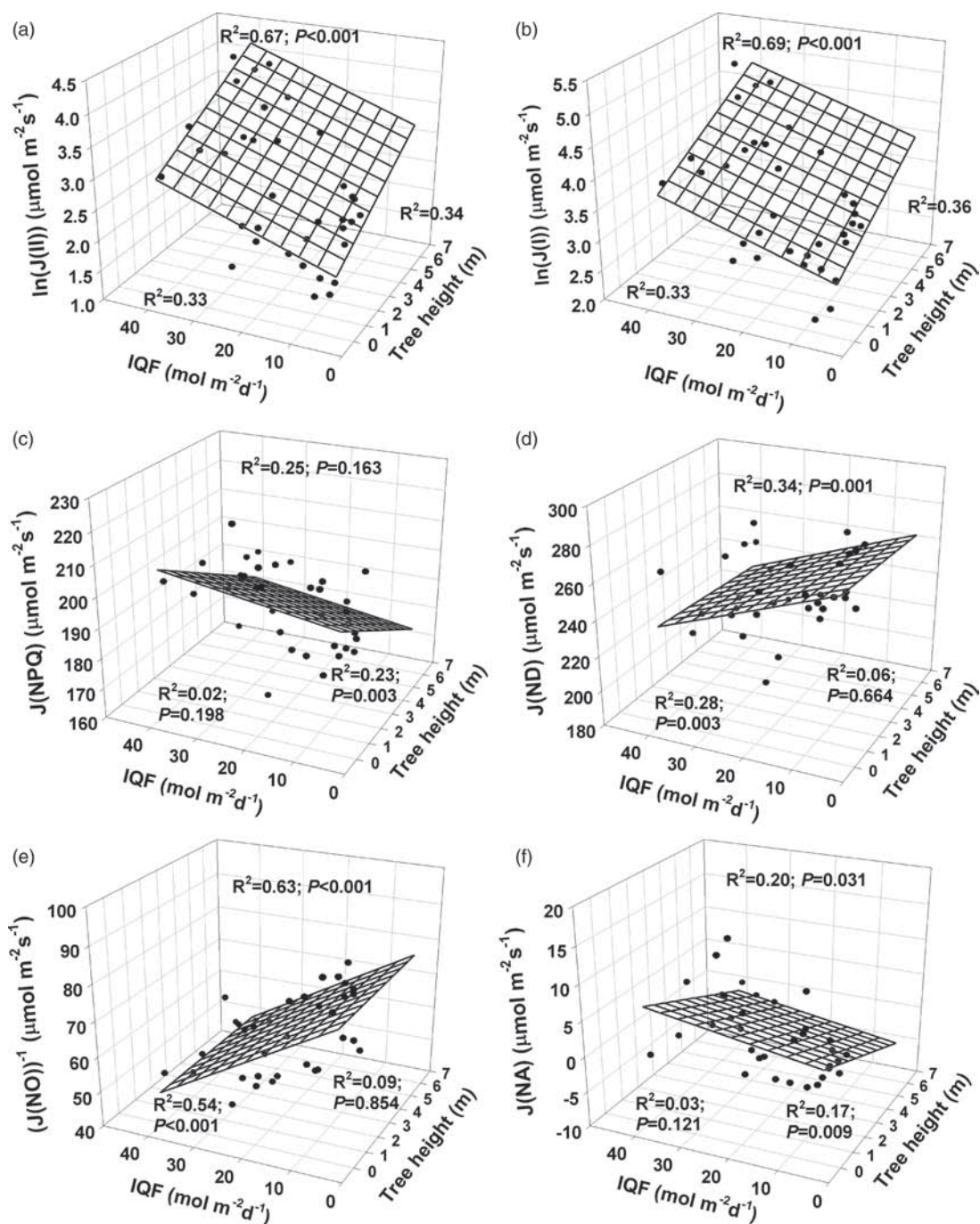


Figure 3. Integrated quantum flux and plant height effects on PSII and PSI light energy flux capacities of *N. nitida* individuals growing in a Chilean evergreen rain forest. (a) Photochemical energy flux through PSII [$J_{(II)}$] and (b) PSI [$J_{(I)}$], (c) ΔpH -xanthophyll-regulated thermal dissipation [$J_{(\text{NPQ})}$], (e) Sum of fluorescence quenching and constitutive thermal dissipation [$J_{(\text{NO})}$], and non-photochemical fluxes consumed by (e) donor [$J_{(\text{ND})}$] and (f) acceptor [$J_{(\text{NA})}$] side limitations. P level of regression, and model and partial determination coefficients are given. Partial P values for IQF and tree size are shown when one variable is non-significant.

remaining fraction of $J_{(II)}$ and $J_{(I)}$ increases ($P < 0.001$), which explained 33% of both (Figure 3a and b). Conversely, PSII non-photochemical energy flux capacity [$J_{(\text{NPQ})}$] was not affected by IQF ($P = 0.198$) and decreased with TH ($P = 0.003$), which explained 23% of its variation (Figure 3c). $J_{(\text{NO})}$ was not affected by TH ($P = 0.854$) and slightly decreased with IQF ($P < 0.001$), which explained 54% of its

variation (Figure 3e). PSI non-photochemical energy flux capacity due to donor side limitations [$J_{(\text{ND})}$] was not affected by TH ($P = 0.664$) and decreased with IQF ($P = 0.003$), which explained 28% of its variation (Figure 3d). $J_{(\text{NA})}$ was not affected by IQF ($P = 0.126$) and decreased with TH ($P = 0.007$), which explained 17% of its variation (Figure 3f).

Table 1. Summaries of multiple regression analysis to test for significant effects of TH and IQF on non-photochemical quenching components of *N. nitida* leaves.

NPQ components	Constant	TH (cm)	IQF (mol photons m ⁻² day ⁻¹)	Model		
				F _{2,6}	P value	R ²
NPQ	3.569***	-0.002 (0.21)*	0.009 (0.35)***	22.420	<0.001	0.56
Sqrt(NPQ _s)	0.900***	-0.000 (0.04)	0.004 (0.03)	1.352	0.272	0.07
NPQ _f	2.726***	-0.001 (0.19)*	-0.047 (0.56)***	52.176	<0.001	0.75
Fr	0.203***	0.000 (0.00)	-0.001 (0.00)	0.156	0.856	0.01

Variance inflation factor (highest VIF = 1.37). Numbers in parentheses indicate the independent determination coefficient (hierarchical partitioning method).

* $P < 0.05$; ** $P < 0.01$; *** $P < 0.001$.

Table 2. Summaries of multiple regression analysis to test for significant effects of tree height and total transmitted radiation on morpho-anatomical traits of *N. nitida* leaves.

Trait	Constant	TH (cm)	TTR (mol photons m ⁻² day ⁻¹)	Model		
				F _{2,6}	P value	R ²
Leaf thickness (μm)	173.210***	0.235 (0.29)***	2.093 (0.29)*	25.072	< 0.001	0.58
Palisade layer thickness (μm)	25.207	0.068 (0.31)***	1.007 (0.31)***	27.917	<0.001	0.62
Spongy mesophyll thickness (μm)	165.398***	-0.124 (0.16)**	0.563 (0.00)	4.226	0.024	0.16
Palisade/spongy mesophyll thickness ¹	5.267***	-0.005 (0.46)**	-0.043 (0.00)	15.480	<0.001	0.46
Palisade cell diameter (μm)	14.407***	-0.006 (0.25)**	-0.082 (0.25)**	17.703	<0.001	0.50
Porosity inside lamina (%)	36.654***	0.004 (0.00)	-0.355 (0.43)***	13.953	<0.001	0.43
Specific leaf area (cm g ⁻¹)	100.036***	-0.009 (0.00)	-1.295 (0.31)**	8.557	0.001	0.31

¹Reciprocal transformation. Variance inflation factor (VIF = 1.37 for all coefficients).

Numbers in parentheses indicate the independent determination coefficient (hierarchical partitioning method).

* $P < 0.05$; ** $P < 0.01$; *** $P < 0.001$.

Effect of IQF and TH on non-photochemical quenching components

Total NPQ lightly increased with IQF and slightly decreased with TH, which together explained 56% of its variation ($P < 0.001$) (Table 1). Besides, total NPQ decreased with TH ($P < 0.024$), which explained 21% of its change. Total NPQ also increased with IQF ($P < 0.001$), which explained 35% of its change. NPQ_s was not affected by either TH ($P = 0.142$) or IQF ($P = 0.183$). NPQ_f decreased with IQF and TH ($P < 0.001$), which together explained 75% of its variation. Besides, NPQ_f was decreased by TH ($P = 0.049$) and IQF ($P < 0.001$), which explained 19 and 56% of its decreases, respectively. Fr was not affected by either TH ($P = 0.627$) or IQF ($P = 0.632$) (Table 1). In order to explore the underlying mechanisms responsible for the observed functional responses on light energy partitioning, a deeper biochemical and morphological characterization was performed (Table 2).

Effect of IQF and TH on foliar morpho-anatomical traits

Leaf thickness increased with IQF and TH, together explaining 61% of its variation ($P < 0.001$). Besides, IQF and TH independently explained 24 and 37% of its increases, respectively (Table 2). Palisade layer thickness increased with IQF and TH, together explaining 64% of its variation ($P < 0.001$). Besides, IQF and TH

independently explained 32 and 32% of its increases, respectively. Spongy mesophyll thickness was not affected by IQF ($P = 0.383$), but decreased with TH ($P = 0.008$), which explained 19% of its variation. Palisade/spongy mesophyll thickness ratio was not affected by IQF ($P = 0.069$), but slightly decreased with TH ($P = 0.001$), which explained 31% of its variation. Palisade cell diameter decreased with IQF and TH, together explaining 53% of its variation ($P < 0.001$). Besides, IQF and TH independently explained 26 and 27% of its increases, respectively. Porosity inside the lamina was not affected by TH ($P = 0.467$), but decreased with IQF ($P < 0.001$), which explained 43% of its variation. Specific leaf area was not affected by TH ($P = 0.735$), but decreased with IQF ($P = 0.002$), which explained 29% of its variation (Table 2).

Effect of IQF and TH on nitrogen, and structural and functional photosynthetic protein contents

We measured the content of the main structural and functional polypeptides of both photosystems as well as total nitrogen. Rubisco content was not related to TH and IQF together ($P = 0.085$). However, Rubisco increased with IQF ($P = 0.026$), which explained 22% of its variation (see Table S5, available as Supplementary Data at *Tree Physiology* Online). Nitrogen increased with IQF and TH ($P < 0.001$),

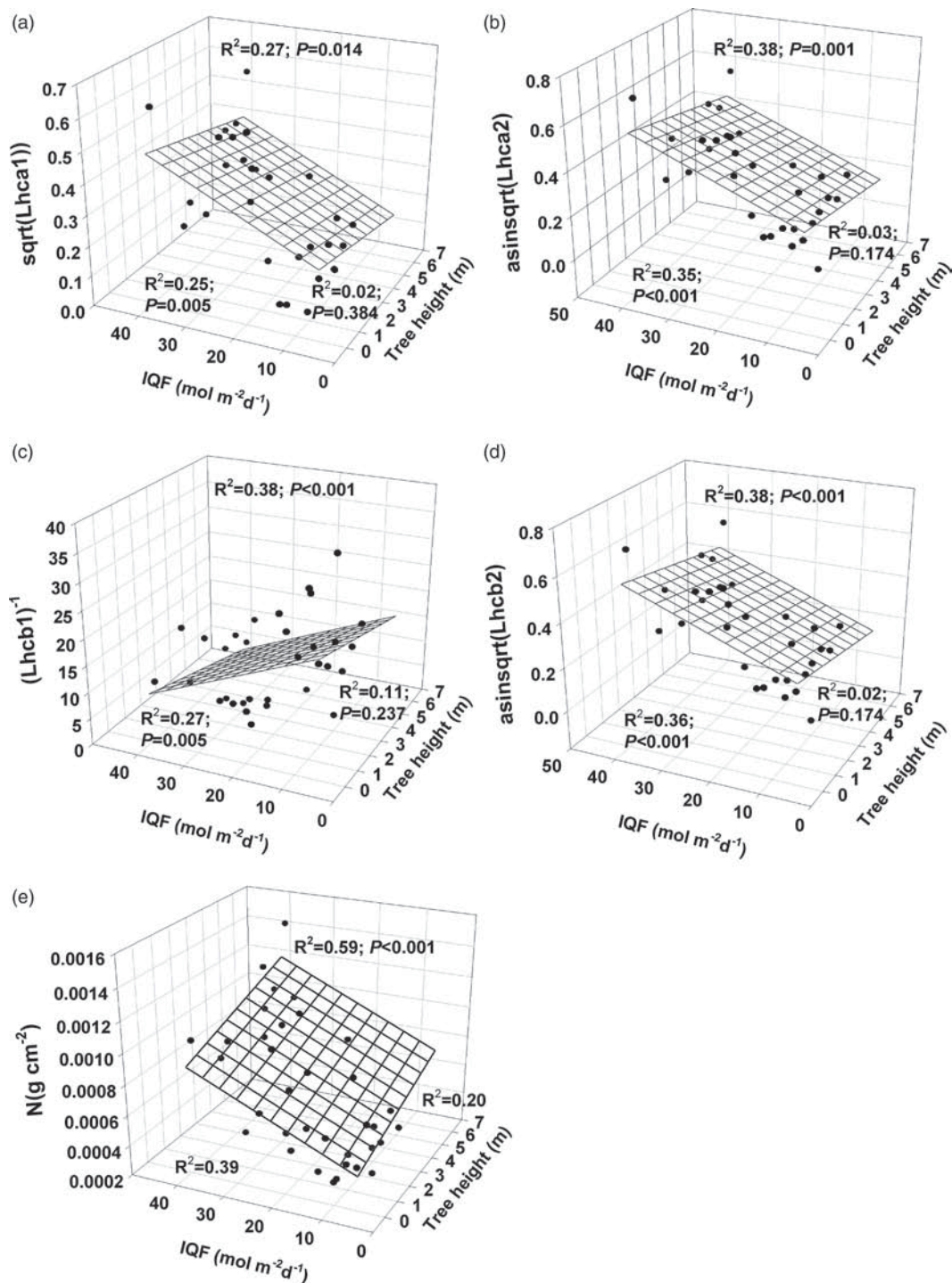


Figure 4. Integrated quantum flux and plant height effects on (a) Lhca1, (b) Lhca2, (c) Lhcb1, (d) Lhcb2 and (e) nitrogen leaf contents of *N. nitida* individuals growing in a Chilean evergreen rain forest. Specific polypeptides were immunodetected and densitometrically measured on western blots. Polypeptides are expressed as relative band intensity cm^{-2} . P level of regression, and model and partial determination coefficients are given. Partial P values for IQF and tree size are shown when one variable is non-significant.

together explaining 59% of its variation. Besides, nitrogen increased with TH ($P = 0.041$) and IQF ($P < 0.001$), which explained 20 and 39% of its increases, respectively (Figure 4e). D1 content was not affected by TH and IQF ($P = 0.163$) (see Table S5, available as Supplementary Data

at *Tree Physiology* Online). PsbS content was not affected by TH and IQF ($P = 0.765$) (see Table S5, available as Supplementary Data at *Tree Physiology* Online). Lhca1, Lhca2, Lhcb1 and Lhcb2 were not affected by TH (lowest $P = 0.174$). Conversely, Lhca1, Lhca2 and Lhcb2 increased

with IQF (highest $P = 0.005$), which explained 25, 35 and 36% of the variations, respectively (Figure 4a–d). Lhcb1 decreased with IQF ($P = 0.005$), which explained 27% of its variation (Figure 4c).

Discussion

As trees grow taller, upper leaves are often progressively exposed to higher vapour pressure deficit and wind speed. These conditions increase water demand as well as hydraulic and gravitational resistance to water flow (Tyree and Ewers 1991, Kull and Niinemets 1993). The above effects commonly result in stomatal and mesophyll limitations that lead to a decrease in CO_2 assimilation (Hubbard et al. 1999, Whitehead et al. 2011) and conditions that favour photoinhibition (Björkman and Powles 1984). Nevertheless, it seems that this size-related limitation depends on the developmental stage of trees (McDowell et al. 2005, Abdul-Hamid and Mencuccini 2009, Whitehead et al. 2011) and on light availability during leaf formation (Thomas and Winner 2002, Terashima et al. 2006). Despite these growth-related limitations, there is emerging evidence showing that there is a compensatory increase in CO_2 uptake. This is, for example, the case for the transition from seedlings to saplings of *M. gigantea* (Ishida et al. 2005), of five dipterocarp (Kenzo et al. 2006) and of four Neotropical species (Rijkers et al. 2000). The parallel developmental and environmental change that woody plants experience during the transition from seedlings to saplings may mask the origin of these compensatory adaptations (Lusk and Warton 2007). In the present study, we clarify the relative contribution of TH and IQF to leaf photosynthetic responses, and morpho-anatomical and biochemical traits by considering a continuous range of tree heights from seedlings to saplings. Despite the expected ontogenetic decrease in tissue and whole plant R_d induced by the enhanced proportion of respiratory versus photosynthetic tissues (Givnish 1988), and by the decrease in the mass contribution of tissues with higher physiological activity and concomitantly higher R_d rates (Machado and Reich 2006), no tree size responses at leaf level R_d were found. The decreases in R_d with increasing plant size have also been indicated by a positive relationship between total R_d and relative growth rates (Poorter et al. 1990, Tjoelker et al. 1999), as well as by negative relationships of both components to plant size. Nevertheless, growth accelerates in most young forests as canopies develop and declines substantially soon after maximum leaf area is attained (Pretzsch 2009). In this study we considered saplings up to 7 m tall; thus the apparent insensibility of R_d to tree size could be caused by the compensatory effect between the ontogenetic decrease in R_d and the increments in growth rates during the seedling–sapling transition and prior to reproductive onset (Thomas 2010).

In *N. nitida*, CO_2 assimilation light response parameters were strongly increased with IQF. The increments in LCP, LSP and A_{max} found with higher IQF could be related to the development of new leaves in more illuminated environments, which may enable them to fully acclimate morpho-anatomically and biochemically to their light environment (Mulkey and Pearcy 1992, Krause et al. 2001, Coopman et al. 2008). This effect was corroborated by the positive response of Rubisco, total nitrogen, LHC polypeptide contents (see Table S5, available as Supplementary Data at *Tree Physiology Online*) and SLA (Table 1) preferentially to IQF. In agreement with Kenzo et al. (2006), our findings showed photosynthetic capacity adjustments to light environment concomitant with changes in leaf morpho-anatomical as well as biochemical properties. Anatomical modifications involved an increase in the thickness of the palisade layer in response to TH and IQF that could be directly involved in the enhancement of carbon assimilation (Niinemets 2006).

The partitioning of absorbed light towards photochemical energy flux in both photosystems [$J_{(\text{II})}$ and $J_{(\text{I})}$] increased independently with TH and IQF. This increase for light energy utilization implies higher potential to safely quench potentially damaging excitation energy via photosynthesis (Demmig and Winter 1988). Consistent with our results, increments in photochemical capacity from seedlings to saplings have been recently reported for several species (Ishida et al. 2005, Kenzo et al. 2006). In contrast, with $J_{(\text{II})}$ the flux of energy dissipated by regulated non-photochemical quenching of absorbed light in PSII [$J_{(\text{NPQ})}$] was slightly diminished with TH and not affected by IQF. The latter indicates that under natural conditions photochemical energy quenching increased in *N. nitida* as trees grew, decreasing their need for thermal dissipation. Hence, the flux of thermally dissipated energy expressed under light saturation conditions remains relatively constant as *N. nitida* plants grow and as foliage explores a more illuminated environment (Coopman et al. 2010). This pattern has also been shown in other species (Ishida et al. 2005). $J_{(\text{NO})}$ was similar between plant sizes and decreased with light availability. In summary, the variation in light energy partitioning in PSII during the seedling to sapling phase of *N. nitida* is referred mainly to photochemical adjustments rather than to non-photochemical ones.

On the other hand, the capacity for non-photochemical quenching due to donor side limitation in PSI [$J_{(\text{ND})}$] was not affected by TH. Conversely, we found an increase in the maximum [$J_{(\text{ND})}$] with lower light availability. This could be caused by the higher photochemical light use capacity of PSI shown by trees growing at higher irradiance, which determines a lower excess of energy for thermal dissipation, or by a lower max $J_{(\text{II})}$ observed in this group of plants compared with max $J_{(\text{I})}$. This apparent imbalance between $J_{(\text{II})}$ and $J_{(\text{I})}$ gets more balanced in plants grown at higher IQF. Non-photochemical energy flux due to acceptor side limitation of PSI [$J_{(\text{NA})}$] reached negligible

levels of around 5, indicating that there was no limitation for NADP+ regeneration and hence no severe biochemical photosynthetic limitations such as carbon diffusion limitation by stomatal closure in leaves of tallest trees (Bond 2000). The hydraulic limitation indicated by Tyree and Ewers (1991) does not seem to be a severe restriction for photosynthetic performance of *nitida* trees up to 7 m tall. The higher increase of $J_{(II)}$ than CO_2 assimilation (A_{max}) in response to TH could be due to the development of alternative electron acceptor pathways, such as photorespiration and the water–water cycle (Johnson 2005), associated with leaves that are exposed to more desiccant conditions, such as those in the medium and upper canopy (taller plants). The previous processes have been recently reported as photochemical photoprotective mechanisms which are up-regulated under stressful conditions that increase photoinhibition susceptibility, such as high light and water deficits (Miyake and Okamura 2003, Miyake et al. 2004).

As indicated before, more illuminated plants possess more efficient mechanisms for photochemical energy utilization at high irradiance than shadier ones (Figure 3a and b). This is consistent with previous reports (Lichtenthaler et al. 2007, Coopman et al. 2008, 2010). Thus a lower fraction of absorbed light energy has to be dissipated as heat. Consistently, the fast-relaxing component (NPQ_f) (which in principle depends on ΔpH and zeaxanthin formation) decreased with IQF (Table 1). In principle, this result seems to be inconsistent with a lack of significant relationship observed between the relative content of PsbS and IQF or TH (see Table S3, available as Supplementary Data at *Tree Physiology* Online). However, reports in *Arabidopsis thaliana* indicate that naturally occurring variation in thermal dissipation is not attributable to PsbS (Niyogi et al. 2005). Additionally, a PsbS-independent non-photochemical quenching has been described (Dall'Osto et al. 2005). Our findings contrast with many other studies that indicate higher thermal dissipation capacities in more illuminated growth environments (Demmig-Adams et al. 1995, Adams et al. 1996). However, it is consistent with strategies reported in evergreen species that inhabit low-temperature environments (Savitch et al. 2000). The changes in zeaxanthin-dependent NPQ did not affect the level of chronic photoinhibition attained, because NPQ_s (indicative of photodamage) remained unchanged with increases in IQF and TH. However, zeaxanthin-dependent NPQ was insufficient to protect the photosynthetic apparatus of *N. nitida* seedlings against photoinhibition, as indicated by NPQ_s , which accounts for around 40% of total NPQ. This result partially disagrees with recent findings in which seedlings of *N. nitida* in summer showed higher levels of photodamage than adult trees (Reyes-Díaz et al. 2009). Nevertheless, the highest level of photodamage reported in this study was equivalent to 25% of total NPQ for seedlings. These differences may be due to the difference in the duration of the photoinhibitory treatment, which in our case was 340% longer. Recently we reported an

ontogenetic shift in the capacity for state transitions (Fr) (Coopman et al. 2008, 2010), where the highest capacity for Fr was obtained in small *N. nitida* seedlings grown in deep-shade conditions ($20 \mu\text{mol photons m}^{-2} \text{s}^{-1}$); this capacity dramatically decreased with light availability and seedling height, indicating that small plants of *N. nitida* grown in low light were better prepared to live in deep-shady environments (Coopman et al. 2008, 2010). Unexpectedly, no variations in Fr were found between tree height and light environment ranges in the present study. Fr has been proposed as a strategy to maximize the efficiency of utilization of absorbed light energy under light limiting conditions for growth (Mullineaux and Emlyn-Jones 2005). In this context, the lowest forest light availability in the study site was not too shaded ($4 \text{ mol photons m}^{-2} \text{ day}^{-1}$, which is equivalent to a PPFD of $100 \mu\text{mol m}^{-2} \text{ s}^{-1}$ during a 12 h photoperiod) in comparison with deep-shade conditions. It seems that Fr is restricted to very early ontogeny of *N. nitida* seedlings growing in deep-shade environments.

Conclusion

Light energy partitioning and leaf morpho-anatomical traits changed with plant size and light availability in *N. nitida*. This was the result of an adaptation to the light environment, but also to an ontogenetic shift in shade tolerance that has been previously reported in this (Coopman et al. 2008, 2010) and in many different tree species (Lusk and Warton 2007). Taller plants can use more efficiently the prevailing high light intensities for photochemistry and CO_2 gain, partially avoiding a possible severe reduction in photosynthetic performance. In this way, the photochemical use of absorbed light was the more plastic photoprotective quenching mechanism which responds to increases in both light availability and TH at the same rate. In contrast, thermal dissipation capacity (NPQ_f) is reduced with higher light availability and pH, maintaining a relatively constant non-photochemically dissipated energy flux within the size and IQF ranges studied in *N. nitida*. The positive stimulatory response of photosynthesis to IQF was based on the parallel modification of morpho-anatomical traits in leaves and on the biochemical reorganization of photosynthetic components. Thus light interception was maximized by the increase in the thickness of the palisade layer, while the components involved in carbon assimilation (Rubisco) and photosystem II were also up-regulated by IQF. The same morphological modifications were observed in response to TH, but they were not enough to induce an enhancement of carbon assimilation. This study highlights the independent effects of plant size and light environment, which contribute in a similar proportion to the increase in photochemical capacities but differentially on the observed changes in photosynthetic responses that characterize the transition from seedling to sapling. Therefore, the major determinant in this transition seems to be the light environment rather than the tree height itself.

Funding

The authors thank FONDECYT 1070551, MICINN BFU B/O24455/09 and PDA-24 for financial support. R.C. was financed by a doctoral and thesis support fellowship granted by CONICYT.

Supplementary data

Supplementary data for this article are available at *Tree Physiology* Online.

References

- Abdul-Hamid, H. and M. Mencuccini. 2009. Age- and size-related changes in physiological characteristics and chemical composition of *Acer pseudoplatanus* and *Fraxinus excelsior* trees. *Tree Physiol.* 29:27–38.
- Adams, W.W., B. Demmig-Adams, D.H. Barker and S. Kiley. 1996. Carotenoids and photosystem II characteristics of upper and lower halves of leaves acclimated to high light. *Aust. J. Plant Physiol.* 23:669–677.
- Alberdi, M., M. Reyes-Díaz, R. Zúñiga, S. Hess, L.A. Bravo and L.J. Corcuera. 2009. Photochemical efficiency of PSII and photoprotective pigments in seedlings and adults of two Proteaceae with different shade tolerance from the Chilean temperate rain forest. *Rev. Chil. Hist. Nat.* 82:387–402.
- Arnon, D. 1949. Copper enzymes in isolated chloroplasts; polyphenol oxidases in *Beta vulgaris*. *Plant Physiol.* 24:1–15.
- Bond, B.J. 2000. Age-related changes in photosynthesis of woody plants. *Trends Plant Sci.* 5:349–353.
- Björkman, O. 1981. Responses to different quantum flux densities. *In* Physiological Plant Ecology. I. Responses to the Physical Environment. Encyclopedia of Plant Physiology. Eds. L. Lange, P.S. Nobel, C.B. Osmond and H. Ziegler. Springer, New York, pp 57–107.
- Björkman, O. and S.B. Powles. 1984. Inhibition of photosynthetic reactions under water stress: interaction with light level. *Planta* 161:490–504.
- Chazdon, R.L. and N. Fetcher. 1984. Photosynthetic light environments in a lowland tropical rain forest in Costa Rica. *J. Ecol.* 72:553–564.
- Chevan, A. and M. Sutherland. 1991. Hierarchical partitioning. *Am. Stat.* 5:90–96.
- Coopman, R.E., M. Reyes-Díaz, V.F. Briceño, L.J. Corcuera, H.M. Cabrera and L.A. Bravo. 2008. Changes during early development in photosynthetic light acclimation capacity explain the shade to sun transition in *Nothofagus nitida*. *Tree Physiol.* 28:1561–1571.
- Coopman, R.E., F. Fuentes-Neira, V.F. Briceño, H.M. Cabrera, L.J. Corcuera and L.A. Bravo. 2010. Light energy partitioning in photosystems I and II during development of *Nothofagus nitida* growing under different light environments in the Chilean evergreen temperate rain forest. *Trees-Struct. Funct.* 24:247–259.
- Dall'Osto, L., S. Caffarri and R. Bassi. 2005. A mechanism of non-photochemical energy dissipation, independent from PsbS, revealed by a conformational change in the antenna protein CP26. *Plant Cell* 17:1217–1232.
- Demmig-Adams, B. and K. Winter. 1988. Light response of CO₂ assimilation, reduction state of Q and radiationless energy dissipation in intact leaves. *Funct. Plant Biol.* 15:151–162.
- Demmig-Adams, B., R.E. Cleland and O. Björkman. 1987. Photoinhibition, 77K chlorophyll fluorescence quenching and phosphorylation of the light-harvesting chlorophyll-protein complex of photosystem II in soybean leaves. *Planta* 172:378–385.
- Demmig-Adams, B., W.W. Adams III, B.A. Logan and A.S. Verhoeven. 1995. Xanthophyll cycle-dependent energy dissipation and flexible photosystem II efficiency in plants acclimated to light stress. *Funct. Plant Biol.* 22:249–260.
- Demmig-Adams, B., W.W. Adams III, D.H. Barker, B.A. Logan, D.R. Bowling and A.S. Verhoeven. 1996. Using chlorophyll fluorescence to assess the fraction of absorbed light allocated to thermal dissipation of excess excitation. *Physiol. Plantarum* 98:253–264.
- Donoso, C. 1993. Bosques templados de Chile y Argentina. Primera edición. Ed. Universitaria, Santiago, Chile, 484 p.
- Ensminger, I., F. Busch and N.P.A. Huner. 2006. Photostasis and cold acclimation: sensing low temperature through photosynthesis. *Physiol. Plantarum* 126:28–44.
- Evans, J.R. 1989. Photosynthesis and nitrogen relationships in leaves of C₃ plants. *Oecologia* 78:9–19.
- Frazer, G.W., C.D. Canham and K.P. Lertzman. 1999. Gap Light Analyzer (GLA), Version 2.0: Imaging software to extract canopy structure and gap light transmission indices from true-colour fisheye photographs, users manual and program documentation. Simon Fraser University, Burnaby, British Columbia, and the Institute of Ecosystem Studies, Millbrook, New York.
- Garnier, E., B. Shipley, C. Roumet and G. Laurent. 2001. A standardized protocol for the determination of specific leaf area and leaf dry matter content. *Funct. Ecol.* 15:688–695.
- Givnish, T.J. 1988. Adaptation to sun shade: a whole-plant perspective. *Aust. J. Plant Physiol.* 15:63–92.
- Grubb, P.J. 1977. The maintenance of species-richness in plant communities: the importance of the regeneration niche. *Biol. Rev.* 52:107–145.
- Hendrickson, L., R. Furbank and W. Chow. 2004. A simple alternative approach to assessing the fate of absorbed light energy using chlorophyll fluorescence. *Photosynth. Res.* 82:73–81.
- Hubbard, R.M., B.J. Bond and M.G. Ryan. 1999. Evidence that hydraulic conductance limits photosynthesis in old *Pinus ponderosa* trees. *Tree Physiol.* 19:165–172.
- Ishida, A., K. Yazaki and A.L. Hoe. 2005. Ontogenetic transition of leaf physiology and anatomy from seedlings to mature trees of a rain forest pioneer tree, *Macaranga gigantea*. *Tree Physiol.* 25:513–522.
- Johnson, G.N. 2005. Cyclic electron transport in C₃ plants: fact or artefact? *J. Exp. Bot.* 56:407–416.
- Kenzo, T., T. Ichie, Y. Watanabe, R. Yoneda, I. Ninomiya and T. Koike. 2006. Changes in photosynthesis and leaf characteristics with tree height in five dipterocarp species in a tropical rain forest. *Tree Physiol.* 26:865–873.
- Kira, T. and K. Yoda. 1989. Vertical stratification in microclimate. *In* Tropical Rain Forest Ecosystems. Eds. H. Lieth and J.A. Werger. Elsevier, Amsterdam, pp 55–71.
- Klughammer, C. and U. Schreiber. 1994. An improved method, using saturating light pulses, for the determination of photosystem I quantum yield via P700+ -absorbance changes at 830 nm. *Planta* 192:261–268.
- Kozłowski, T.T. 2002. Physiological ecology of natural regeneration of harvested and disturbed forest stands: implications for forest management. *Forest Ecol. Manag.* 58:195–221.
- Kramer, D., G. Johnson, O. Kiirats and G. Edwards. 2004. New fluorescence parameters for the determination of Q_A redox state and excitation energy fluxes. *Photosynth. Res.* 79:209–218.
- Krause, G.H., O.Y. Koroleva, J.W. Dalling and K. Winter. 2001. Acclimation of tropical tree seedlings to excessive light in simulated tree-fall gaps. *Plant Cell Environ.* 24:1345–1352.

- Kull, O. and Ü. Niinemets. 1993. Variations in leaf morphometry and nitrogen concentration in *Betula pendula* Roth., *Corylus avellana* L. and *Lonicera xylosteum* L. *Tree Physiol.* 12:311–318.
- Laemmli, U.K. 1970. Cleavage of structural proteins during the assay of the head of bacteriophage T4. *Nature.* 227:680–685.
- Lambers, H., F.S. Chapin III and T.L. Pons. 2008. *Plant physiological ecology*, 2nd edn. Springer, New York, 604 p.
- Larcher, W. 2003. *Physiological plant ecology*, 4th edn. Springer, Berlin, 513 p.
- Lawlor, D. 2001. *Photosynthesis*, 3rd edn. Springer, New York, 386 p.
- Lichtenthaler, H., F. Babani and G. Langsdorf. 2007. Chlorophyll fluorescence imaging of photosynthetic activity in sun and shade leaves of trees. *Photosynth. Res.* 93:235–244.
- Lunde, C., P.E. Jensen, A. Haldrup, J. Knoetzel and H.V. Scheller. 2000. The PSI-H subunit of photosystem I is essential for state transitions in plant photosynthesis. *Nature* 408:613–615.
- Lusk, C.H. and D.I. Warton. 2007. Global meta-analysis shows that relationships of leaf mass per area with species shade tolerance depend on leaf habit and ontogeny. *New Phytol.* 176:764–774.
- Lusk, C.H., R.L. Chazdon and G. Hofmann. 2006. A bounded null model explains juvenile tree community structure along light availability gradients in a temperate rain forest. *Oikos* 112:131–137.
- Lusk, C.H., D.S. Falster, C.K. Jara-Vergara, M. Jimenez-Castillo and A. Saldaña-Mendoza. 2008. Ontogenetic variation in light requirements of juvenile rainforest evergreens. *Funct. Ecol.* 22:454–459.
- Machado, J.-L. and P.B. Reich. 2006. Dark respiration rate increases with plant size in saplings of three temperate tree species despite decreasing tissue nitrogen and nonstructural carbohydrates. *Tree Physiol.* 26:915–923.
- Markwell, J., J. Osterman and J. Mitchell. 1995. Calibration of the Minolta SPAD-502 leaf chlorophyll meter. *Photosynth. Res.* 46:467–472.
- McDowell, N.G., J. Licata and B.J. Bond. 2005. Environmental sensitivity of gas exchange in different-sized trees. *Oecologia* 145:9–20.
- Meziane, D. and B. Shipley. 2001. Direct and indirect relationships between leaf area, leaf nitrogen and leaf gas exchange. Effects of irradiance and nutrient supply. *Ann. Bot.* 88:915–927.
- Miyake, C. and M. Okamura. 2003. Cyclic electron flow within PSII protects PSII from its photoinhibition in thylakoid membranes from Spinach chloroplasts. *Plant Cell Physiol.* 44:457–462.
- Miyake, C., Y. Shinzaki, M. Miyata and K.i. Tomizawa. 2004. Enhancement of cyclic electron flow around PSI at high light and its contribution to the induction of non-photochemical quenching of Chl fluorescence in intact leaves of tobacco plants. *Plant Cell Physiol.* 45:1426–1433.
- Mulkey, S.S. and R.W. Pearcy. 1992. Interactions between acclimation and photoinhibition of photosynthesis of a tropical forest understorey herb, *Alocasia macrorrhiza*, during simulated canopy gap formation. *Funct. Ecol.* 6:719–729.
- Mullineaux, C.W. and D. Emlin-Jones. 2005. State transitions: an example of acclimation to low-light stress. *J. Exp. Bot.* 56:389–393.
- Niinemets, U. 2006. The controversy over traits conferring shade-tolerance in trees: ontogenetic changes revisited. *J. Ecol.* 94:464–470.
- Niyogi, K.K., X.P. Li, V. Rosenberg and H.S. Jung. 2005. Is PsbS the site of non-photochemical quenching in photosynthesis? *J. Exp. Bot.* 56:375–382.
- Pascal, A.A., Z. Liu, K. Broess, B. van Oort, H. van Amerongen, C. Wang, P. Horton, B. Robert, W. Chang and A. Ruban. 2005. Molecular basis of photoprotection and control of photosynthetic light-harvesting. *Nature* 436:134–137.
- Poorter, H., C. Remkes and H. Lambers. 1990. Carbon and nitrogen economy of 24 wild species differing in relative growth rate. *Plant Physiol.* 94:621–627.
- Poorter, L., F. Bongers, F.J. Sterck and H. Woll. 2005. Beyond the regeneration phase: differentiation of height-light trajectories among tropical tree species. *J. Ecol.* 93:256–267.
- Pretzsch, H. 2009. *Forest dynamics, growth and yield*. Springer, Berlin, 664 p.
- Quinn, G.P. and M.J. Keough. 2006. *Experimental design and data analysis for biologists*. Cambridge University Press, Edinburgh, 537 p.
- Reich, P.B. 2001. Body size, geometry, longevity and metabolism: do plant leaves behave like animal bodies? *Trends Ecol. Evol.* 16:674–680.
- Reyes-Díaz, M., A.G. Ivanov, N.P.A. Huner, M. Alberdi, L.J. Corcuera and L.A. Bravo. 2009. Thermal energy dissipation and its components in two developmental stages of a shade-tolerant species, *Nothofagus nitida*, and a shade-intolerant species, *Nothofagus dombeyi*. *Tree Physiol.* 29:651–662.
- Richardson, A.D., S.P. Duigan and G.P. Berlyn. 2002. An evaluation of non-invasive methods to estimate foliar chlorophyll content. *New Phytol.* 153:185–194.
- Rijkers, T., T.L. Pons and F. Bongers. 2000. The effect of tree height and light availability on photosynthetic leaf traits of four neotropical species differing in shade tolerance. *Funct. Ecol.* 14:77–86.
- Sadzawka, A., R. Grez, M.L. Mora, N. Saavedra, M. Carrasco, H. Flores and C. Rojas. 2004. *Métodos de análisis de tejidos vegetales*. Comisión de Normalización y Acreditación (CNA), Sociedad Chilena de la Ciencia del Suelo, Chile, 35 p.
- Savitch, L.V., A. Massacci, G.R. Gray and N.P.A. Huner. 2000. Acclimation to low temperature or high light mitigates sensitivity to photoinhibition: roles of the Calvin cycle and the Mehler reaction. *Aust. J. Plant Physiol.* 27:253–264.
- Schreiber, U., U. Schliwa and W. Bilger. 1986. Continuous recording of photochemical and non-photochemical chlorophyll fluorescence quenching with a new type of modulation fluorometer. *Photosynth. Res.* 10:51–62.
- Sokal, R.R. and J.F. Rohlf. 1995. *Biometry: The principles and practice of statistics in biological research*. W. H. Freeman and Company, New York, 887 p.
- Spangfort, M. and B. Andersson. 1989. Subpopulations of the main chlorophyll a/b light harvesting complex of photosystem II – isolation and biochemical characterization. *Biochim. Biophys. Acta* 977:163–170.
- Terashima, I., Y.T. Hanba, Y. Tazoe, V. Poonam and S. Yano. 2006. Irradiance and phenotype: comparative eco-development of sun and shade leaves in relation to photosynthetic CO₂ diffusion. *J. Exp. Bot.* 57:343–354.
- Thomas, S.C. 2010. Photosynthetic capacity peaks at intermediate size in temperate deciduous trees. *Tree Physiol.* 30:555–573.
- Thomas, S.C. and W.E. Winner. 2002. Photosynthetic differences between saplings and adult trees: an integration of field results by meta-analysis. *Tree Physiol.* 22:117–127.
- Tjoelker, M.G., P.B. Reich and J. Oleksyn. 1999. Changes in leaf nitrogen and carbohydrates underlie temperature and CO₂ acclimation of dark respiration in five boreal tree species. *Plant Cell Environ.* 22:767–778.
- Tyree, M.T. and F.W. Ewers. 1991. *The hydraulic architecture of trees and other woody plants*. *New Phytol.* 119:345–360.

- Veblen, T.T., C. Donoso and T. Kitsberger. 1996. Ecology of southern Chilean and Argentinean *Nothofagus* forests. *In* The Ecology and Biogeography of *Nothofagus* Forests. Eds. T.T. Veblen, R. Hill and J. Read. Yale University Press, New Haven, pp 293–353.
- Walters, R.G. and P. Horton. 1991. Resolution of components of non-photochemical chlorophyll fluorescence quenching in barley leaves. *Photosynth. Res.* 27:121–133.
- Whitehead, D., M.M. Barbour, K.L. Griffin, M.H. Turnbull, and D.T. Tissue. 2011. Effects of leaf age and tree size on stomatal and mesophyll limitations to photosynthesis in mountain beech (*Nothofagus solandrii* var. *cliffortioides*). *Tree Physiol.* 9:985–996.
- Wright, J., P.B. Reich, M. Westoby, *et al.* 2004. The worldwide leaf economics spectrum. *Nature* 428:821–827.